NAVAL POSTGRADUATE SCHOOL
MONTEREY, CALIFORNIA

THESIS

DTIC QUALITY INSPECTED 4

OCEAN WAVE DATA ANALYSIS USING HILBERT TRANSFORM TECHNIQUES

by

Moisés M. Navarro
December, 1996

Thesis Advisor: Andrés Larraza
Co-Advisor: Roberto Cristi

Approved for public release; distribution is unlimited.

19970919 033

REPORT DOCUMENTATION PAGE		Form Approved OMB No. 0704-0188

Public reporting burden for this collection of information is estimated to average 1 hour per response, including the time for reviewing instruction, searching existing data sources, gathering and maintaining the data needed, and completing and reviewing the collection of information. Send comments regarding this burden estimate or any other aspect of this collection of information, including suggestions for reducing this burden, to Washington Headquarters Services, Directorate for Information Operations and Reports, 1215 Jefferson Davis Highway, Suite 1204, Arlington, VA 22202-4302, and to the Office of Management and Budget, Paperwork Reduction Project (0704-0188) Washington DC 20503.

1. AGENCY USE ONLY	2. REPORT DATE December, 1996.	3. REPORT TYPE AND DATES COVERED Master's Thesis

4. TITLE AND SUBTITLE OCEAN WAVE DATA ANALYSIS USING HILBERT TRANSFORM TECHNIQUES	5. FUNDING NUMBERS
6. AUTHOR Moisés Navarro López Lieutenant Commander, Venezuelan Navy	

7. PERFORMING ORGANIZATION NAME AND ADDRESS Naval Postgraduate School Monterey CA 93943-5000	8. PERFORMING ORGANIZATION REPORT NUMBER
9. SPONSORING/MONITORING AGENCY NAME(S) AND ADDRESS(ES) Naval Postgraduate School Monterey CA 93943-5000	10. SPONSORING/MONITORING AGENCY REPORT NUMBER

11. SUPPLEMENTARY NOTES The views expressed in this thesis are those of the author and do not reflect the official policy or position of the Department of Defense or the U.S. Government.

12a. DISTRIBUTION/AVAILABILITY STATEMENT Approved for public release; distribution is unlimited.	12b. DISTRIBUTION CODE

13. ABSTRACT

A novel technique to determine the phase velocity of long-wavelength shoaling waves is investigated. Operationally, the technique consists of three steps. First, using the Hilbert transform of a time series, the phase of the analytic signal is determined. Second, the correlations of the phases of analytic signals between two points in space are calculated and an average time of travel of the wave fronts is obtained. Third, if directional spectra are available or can be determined from time series of large array of buoys, the angular information can be used to determine the true time of travel. The phase velocity is obtained by dividing the distance between buoys by the correlation time. Using the Hilbert transform approach, there is no explicit assumption of the relation between frequency and wavenumber of waves in the wave field, indicating that it may be applicable to arbitrary wave fields, both linear and nonlinear. Limitations of the approach are discussed.

14. SUBJECT TERMS Hilbert Transform, Sea waves, Cross-correlations			15. NUMBER OF PAGES 52
			16. PRICE CODE

17. SECURITY CLASSIFICATION OF REPORT Unclassified	18. SECURITY CLASSIFICATION OF THIS PAGE Unclassified	19. SECURITY CLASSIFICATION OF ABSTRACT Unclassified	20. LIMITATION OF ABSTRACT UL

NSN 7540-01-280-5500

Standard Form 298 (Rev. 2-89)
Prescribed by ANSI Std. 239-18 298-102

OCEAN WAVE DATA ANALYSIS USING HILBERT TRANSFORM TECHNIQUES

Moisés M. Navarro
Lieutenant Commander, Venezuelan Navy
B.S., Venezuelan Naval School, 1982

Submitted in partial fulfillment
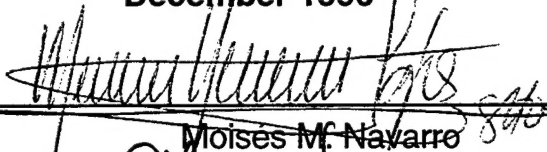of the requirements for the degree of

MASTER OF SCIENCE IN APPLIED PHYSICS
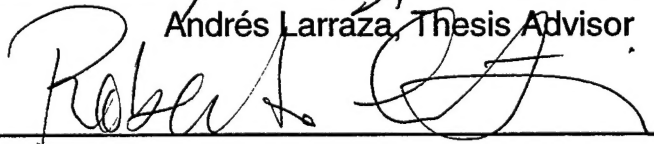
from the
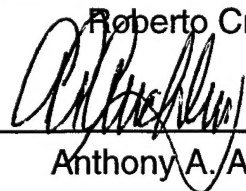
NAVAL POSTGRADUATE SCHOOL
December 1996

Author: _____
Moisés M. Navarro

Approved by: _____
Andrés Larraza, Thesis Advisor

_____
Roberto Cristi, Co-Advisor

_____
Anthony A. Atchley , Chairman
Department of Physics

ABSTRACT

A novel technique to determine the phase velocity of long-wavelength shoaling waves is investigated. Operationally, the technique consists of three steps. First, using the Hilbert transform of a time series, the phase of the analytic signal is determined. Second, the correlations of the phases of analytic signals between two points in space are calculated and an average time of travel of the wave fronts is obtained. Third, if directional spectra are available or can be determined from time series of large array of buoys, the angular information can be used to determine the true time of travel. The phase velocity is obtained by dividing the distance between buoys by the correlation time. Using the Hilbert transform approach, there is no explicit assumption of the relation between frequency and wavenumber of waves in the wave field, indicating that it may be applicable to arbitrary wave fields, both linear and nonlinear. Limitations of the approach are discussed.

TABLE OF CONTENTS

ACKNOWLEDGMENTS

x

I. INTRODUCTION

As ocean waves shoal, the wave field evolves substantially from its deep water state. While the geometry of the dynamic currents and of the bottom topography determine the direction and to some extent the energy of the spectral components, nonlinearities in the wave field lead to harmonic generation and to spectrum broadening. Furthermore, for a nonlinear wave field, there is an apparent negative refraction of the spectral peak (Abreu et al. 1992). Thus, for a known sloping bottom, the refraction away from the beach normal is a direct consequence of nonlinear energy transfer. On the other hand, linear theory does not predict most of these changes, and for a given shoaling spectrum, linear theory might lead to an incorrect determination of the beach normal.

Directional spectrum has become commonly used to describe nonlinear random ocean waves because it provides ways to estimate the significant wave heights in a breaker and also to determine the predominant direction for net sediment transport. Considerable progress has been made over the last two decades to study the evolution of the wave spectrum due to refraction, diffraction, and nonlinear interaction under conditions of mild slope (Lui et al. 1985, Freilich and Guza 1984, Abreu et al. 1992). However, field conditions often violate the basic assumption that the wavelength be smaller than the characteristic length scale of bottom variations. Nevertheless, it can be shown (Larraza, 1994) that using a ray optics approximation, the determination of the kinematic wave parameters (wavelength, direction of propagation) for a given

1

geometry is within 5% of its true value. On the other hand, the determination of the dynamic values (energy, momentum) exceeds at least 15% the true value. Thus by using ray theory, sediment transport and other relevant effects caused by the wave's momentum will be ill estimated.

For an arbitrary bottom topography, wave energy and momentum can be calculated within the physical optics approximation. The passage from geometrical to physical optics can in principle be accomplished by use of a path integral formulation approach. Within this formulation, the basis states are characterized by the "rays", and the physical optics results from a sum over all the possible paths (and not only the path determined by Fermat's principle). The path integral formulation approach has not been considered previously either for gravity waves over a changing topography or for shoaling waves. This situation is particularly surprising because the problem can be stated from the onset by using the known results of ray optics, either linear or nonlinear, and performing a sum over all possible ray paths of the basis states. Even though there are standard analytical techniques to deal with certain special cases, the most general ones can only be solved numerically.

Because the sea floor is known to be a controlling factor in low-frequency shallow water wave propagation (Akal, 1980, Akal and Jensen 1983), phase velocity measurements can in principle be used to determine bottom topography, which can in turn be used for true ground determination in remote sensing applications. The inverse problem, that is, the determination of the topography given the evolution of the spectrum along a path requires an accurate technique

to determine celerity and direction of the waves in a given wave field data. Common techniques of Fourier transform are usually inadequate. In the Fourier transform, a real space-time signal is converted to a complex frequency-wavevector signal. Thus, for applications to ocean wave field data a dispersion relation between frequency and wavenumber has to be assumed in order to determine the phase velocity of the spectral components. The problem can be complicated by nonlinearities in the wave field.

On the other hand, the Hilbert transform of a real valued time-space signal is another real value time-space signal for which the phase of a signal can be calculated in terms of the signal itself and its Hilbert transform. Thus by using the time series of a signal measured at different points, one can determine a relative phase shift and extract phase velocity measurements without reference to a dispersion relation.

In this thesis we present an analysis of ocean surface waves data obtained by The Naval Research Laboratory Stennis Center, in support of Hamlet's Cove I (Smith, 1994). An immediate goal is to extract phase velocity information from time series at three buoys. The data analysis technique used throughout this thesis is based on the Hilbert transform. This technique allow us to get local properties, local energy and local frequency, of the signal instead of the global properties that others techniques, like the Fourier transform, would give (Long, 1995).

In Chapter II we give a brief introduction to linear water waves and point out their dispersive character. We also present a description of the local

topography for the wave data that we analyze and emphasize the need for an inverse problem in arbitrary topographies. Chapter III gives a detailed account of the basic ideas involved in Hilbert transforms. In Chapter IV we present the results and the procedures used for the analysis of the data. The data was analyzed using the Fast Fourier Transform (FFT), the Hilbert transform, and the cross-correlation functions of MATLAB. In Chapter V we discuss the results and provide some recommendations for future work.

II. SURFACE WAVES IN THE HAMLET'S COVE I EXPERIMENT

In the first part of this chapter, we present a brief introduction to surface gravity waves over uniform depth and emphasize their dispersive behavior. In contrast, the data that we analyze throughout this thesis is over nonuniform terrain. The second part of this chapter gives a detailed description of the local topography for the Hamlet's Cove I experiment.

A. SURFACE WAVES IN WATER

When a group of waves moves across the surface of water, each particular wavecrest travels faster than the group as a whole, and eventually passes through it. Thus new crest continually are being created at the back of the group while old crests are disappearing at the front.

This behavior does occur because water waves are dispersive. We can say that this implies that the different Fourier components that make the general disturbance have phase velocities that depend on their wavelength. For surface waves, if the surface elevation of water with uniform depth h is described by the wavetrain

$$\eta = A \cos (kx - \omega t) \qquad , \qquad (1.1)$$

the wave speed is given by

$$c = \omega \, / \, k = \left(\frac{g}{k} \tanh(kh) \right)^{1/2} \quad , \tag{1.2}$$

so that waves of longer wavelength, $\lambda = 2\pi \, / \, k$, travel faster. In Eq (1.1) k is the wavenumber and ω is the frequency of the wave.

While each individual wavecrest travels with speed c, the velocity of travel of the group as a whole is the group velocity

$$c_g = d\omega \, / \, dk \quad . \tag{1.3}$$

The phase velocity in water with uniform depth h (Acheson, 1995) can not exceed $\sqrt{gh}$. For kh large, i.e. $h \gg \lambda$, $\tanh(kh) \cong 1$, and

$$c^2 \cong g \, / \, k \quad , \tag{1.4}$$

corresponding to the case of infinite depth. A good approximation for deep water waves is for depths h greater than about $\frac{1}{3}\lambda$. In shallow water, i.e. $h \ll \lambda \, / \, 2\pi$, $\tanh(kh) \cong kh$, and equation (1.2) becomes

$$c^2 \cong gh \quad . \tag{1.5}$$

This equation is important, because as we can see c is independent of k for shallow water. As we will see, the data analyzed in this thesis is remarkably nondispersive.

B. HAMLET'S COVE TOPOGRAPHY

The data analyzed in this thesis is from three bottom-mounted pressure gauge/ current meters for the measurements correspond to directional wave spectra, currents, and tidal elevation. The gauges were deployed in depths of 10' , 15', and 25' installed in support of Hamlet Cove I experiment.

The three bottom-mounted pressure gauges were placed on either side of the sand bar as shown in Figures 2.1 and 2.2
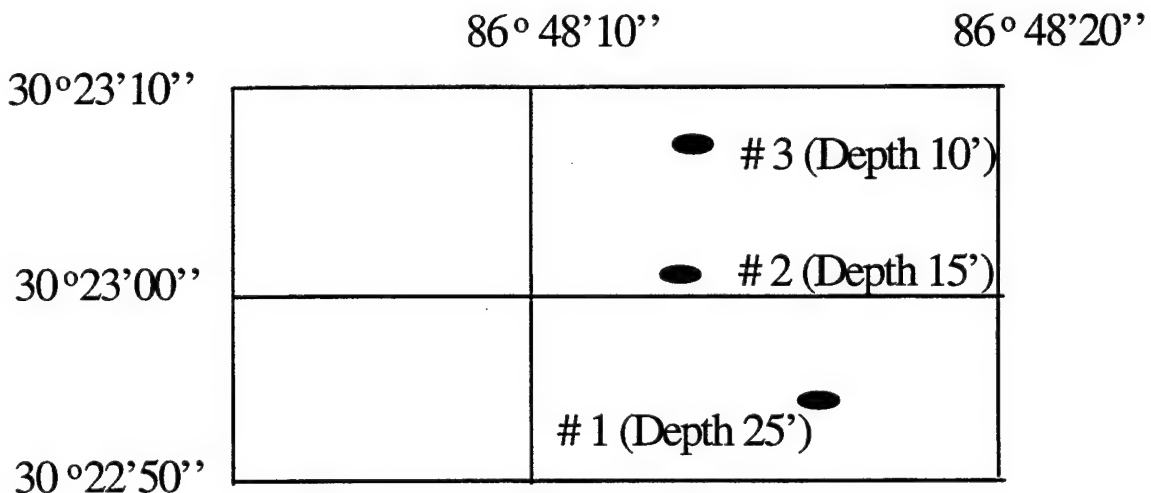

Figure 2.1. Coordinates for the Positions of the gauges and their depths in feet.

7
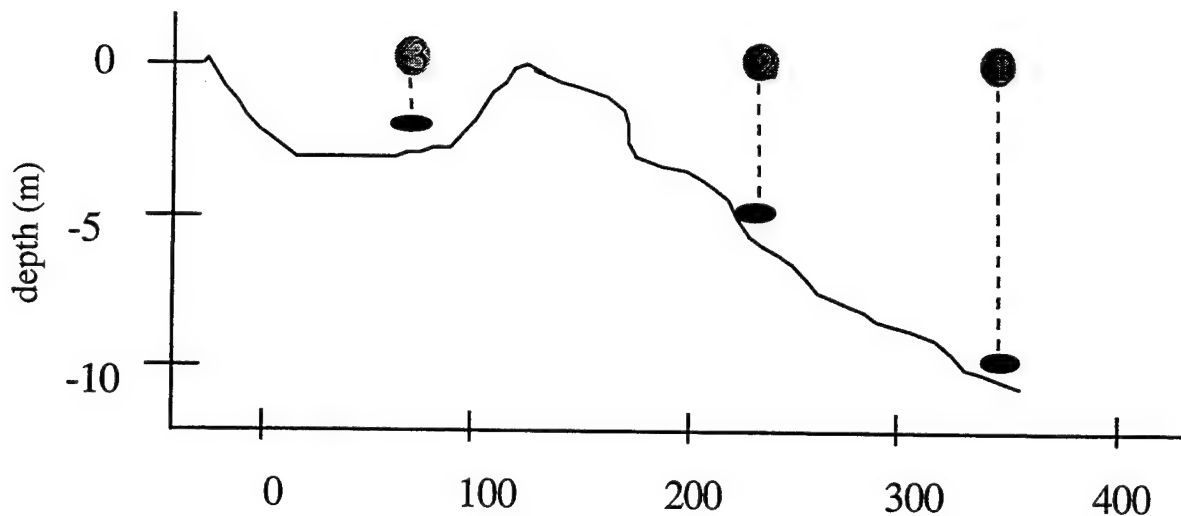
Figure 2.2. Distance from shore (m) of the three buoys and reference to the sand bar. The sand bar profile, measured relative to the surface, is a t a depth of 1.3 m 150 m off shore.

The buoys used collected data from the wave as pressure, x-component of the velocity and the y-component as well. The sampling was continuous with a sampling frequency of 2 Hz .

Because the pressure gauge responds to the rise and fall to the free surface, the pressure at depth z attenuates by a factor proportional to e^{-kz} where k is $2\pi/\lambda$ and λ is the wavelength of the Fourier component of the surface disturbance. At the 15' and 25' depths, (gauges 1 and 2) frequencies above 0.3 Hz were below the noise level of the instruments and, therefore, were ignored in the analysis. The high frequency cut-off for gauge number 3 is 0.5 Hz. Table 2-1 shows the data collection periods for each instrument. We analyzed the data collected by the three buoys in 16 July 1994.

8

Gauge	1	2	3
DATES	14 JUL-20 JUL	14 JUL- 20 JUL	14 JUL- 20 JUL
	20 JUL-29 JUL	20 JUL- 29 JUL	20 JUL- 29 JUL
	29 JUL-1 AUG	29 JUL- 3 AUG	29 JUL- 3 AUG
	3 AUG-10 AUG	3 AUG-10 AUG	3 AUG-9 AUG
	12 AUG-17 AUG	10 AUG-17 AUG	FAILED
	18 AUG-24 AUG	18 AUG-24 AUG	17AUG-24 AUG
	24 AUG-4 SEP	FAILED	FAILED

Table 2-1   Dates for the data collected at the three buoys. The data analyzed in this thesis corresponds to data collected on 16 July 1994.

From the bathymetry survey shown in Figure 2.2, we can see that refraction and diffraction effects from waves 60 m long and longer may be used to characterize the bottom topography. This long waves, due mainly to swell, are essentially nondispersive and already violate the conditions for ray optics to apply.   Because shorter dispersive waves are mainly due to local winds, they would not give accurate topography estimates. Thus, phase velocity estimates from the long waves are the first step to determine an unknown bathymetry.

III. THE HILBERT TRANSFORM

In this chapter we review some of the basic concepts of the Hilbert transform, following the review article by Bendat (1989). In order to elucidate the concept and possible applications of the Hilbert transform, we present three equivalent definitions, namely as a convolution integral, as a $\pi/2$ phase shifter, and as an imaginary part of an analytic signal.

The Hilbert Transform of a real valued signal is a complex signal called the analytic signal. The real part of the analytic signal is the original real-valued time signal while the imaginary part is a copy of the original signal with each of its Fourier components shifted in phase by 90 (Bendat, 1989). The transformed signal retains the same amplitude and frequency information contained in the original signal with the added phase information dependent on the phase of the original data.

For any real time series, $\zeta(t)$, the Hilbert transform $\xi(t)$ is

$$\xi(\tau) = \frac{1}{\pi} P \int_{-\infty}^{+\infty} \frac{\zeta(t)}{\tau - t} dt \qquad , \qquad (3.1)$$

in which P implies the principal value. The analytic continuation of the Hilbert transform is thus the Cauchy integral which corresponds to translations of an analytic function in the complex domain of integration.

The analytic signal $Z(t)$ is the real based time series defined by

11

$$Z(t) = \zeta(t) + j\,\xi(t) \qquad , \qquad (3.2)$$

which can also be written as

$$Z(t) = A(t)\,e^{\,j\vartheta(t)} \qquad , \qquad (3.3)$$

where A(t) is called the envelope signal or the amplitude and $\vartheta(t)$ is called the instantaneous phase signal, defined by:

$$A(t) = [\zeta^2(t) + \xi^2(t)]^{1/2}, \qquad (3.4)$$

and

$$\vartheta(t) = \tan^{-1}[\xi(t)\,/\,\zeta(t)], \qquad (3.5)$$

respectively. The instantaneous frequency ω is given by

$$\omega = \frac{d\vartheta(t)}{dt} \qquad , \qquad (3.6)$$

and the local energy is one half of the square value of the amplitude. Eqs. (3.4), (3.5), and (3.6) represents local properties in time.

The properties of the Hilbert Transform can be best understood in terms of three equivalent definitions.

1)   Definition as Convolution Integral

The Hilbert Transform of a real valued function $\zeta(t)$ extending from $-\infty < t < +\infty$ is a real valued function as described in (3.1):

$$\xi(\tau) = H[\zeta(t)] = \frac{1}{\pi} P \int_{-\infty}^{\infty} \frac{\zeta(t)}{(\tau - t)} dt \quad , \tag{3.7}$$

thus $\xi(t)$ is the convolution integral of $\zeta(t)$ with $(1 / \pi t)$, written as

$$\xi(t) = \zeta(t) * \left(\frac{1}{\pi t} \right) \quad . \tag{3.8}$$

2) Definition as $(\pi / 2)$ Phase Shift System

If $F'(f)$ is the Fourier transform of $\xi(t)$, namely

$$F'(f) = \int_{-\infty}^{+\infty} \xi(t) e^{-j2\pi ft} dt , \tag{3.9}$$

then, from the convolution property of the Hilbert transform (Bendat, 1989) and equation (3.7), it follows that $F'(f)$ is the Fourier transform of $\zeta(t)$, multiplied by the Fourier transform of $(1 / \pi t)$ where

$$\int_{-\infty}^{+\infty} \frac{e^{-j2\pi ft}}{\pi t} dt = -j \operatorname{sgn} f = \begin{cases} -j \text{ for } f > 0 \\ j \text{ for } f < 0 \end{cases} \tag{3.10}$$

Hence, equation (3.6) is equivalent to the passage of $\zeta(t)$ through a system defined by $(-j \operatorname{sgn} f)$ to yield:

$$F'(f) = (-j \operatorname{sgn} f) F''(f) \quad , \tag{3.11}$$

where $F''(f)$ is the Fourier transform of $\zeta(t)$. The complex-valued quantity $F'(f)$ is the Hilbert transform of the complex-valued quantity $F''(f)$ as defined by:

$$F'(f) = H[F''(f)] = (-j\,\text{sgn} f)\, F''(f) \qquad . \qquad (3.12)$$

The Fourier transform $(-j\,\text{sgn} f)$ can be represented by

$$B(f) = -j\,\text{sgn} f = \begin{cases} e^{-j(\pi/2)} & \text{for } f > 0 \\ e^{\,j(\pi/2)} & \text{for } f < 0 \end{cases} \qquad , \qquad (3.13)$$

or using the complex polar notation

$$B(f) = |B(f)|\, e^{-j\phi_b(f)}, \qquad (3.14)$$

Hence, $B(f)$ is a $(\pi/2)$ phase shift system where

$$|B(f)| = 1 \text{ for all } f, \qquad (3.15)$$

and

$$\phi_b(f) = \begin{cases} \pi/2 & \text{for } f > 0 \\ -\pi/2 & \text{for } f < 0 \end{cases}, \qquad (3.16)$$

Thus if one writes:

$$F''(f) = |F''(f)|\, e^{-j\phi_x(f)}, \qquad (3.17)$$

14

it follows that

$$F'(f) = |F'(f)| \, e^{-j\varphi_x(f)} = |F''(f)| \, e^{-j\left|\varphi_x(t)+\varphi_b(t)\right|} , \qquad (3.18)$$

Thus the Hilbert transform consist of passing $\zeta(t)$ through a system which leaves the magnitude of $F''(f)$ unchanged, but changes the phase from $\phi_x(f)$ to $\phi_x(f) + \phi_b(f)$. Thus

$$\varphi_x(f) \rightarrow \varphi_x(f) + (\pi/2) \quad \text{for } f > 0 \ , \qquad (3.19a)$$

$$\varphi_x(f) \rightarrow \varphi_x(f) - (\pi/2) \quad \text{for } f < 0 \qquad (3.19b)$$

in other words, the Hilbert transform shifts by $\pi/2$ for positive frequencies and by $-\pi/2$ for negative frequencies.

3)   Definition as Imaginary part of Analytic Signal

A third useful way to understand and to compute the Hilbert transform is to introduce the analytic signal $Z(t)$ which allows us to work with the amplitude $A(t)$, and the phase $\phi(t)$ equations (3.4 and 3.5). Time derivatives of the phase yield the instantaneous frequency ω (3.6).

Examples of Hilbert transforms and the corresponding Fourier transform of some simple functions are shown in Figure 3.1. The convolution and phase shifts due to the Hilbert transform are apparent. Also apparent is the fact that the analytic signal preserves local amplitude.

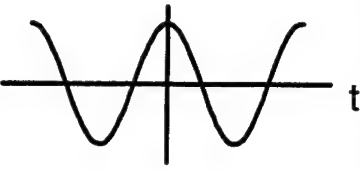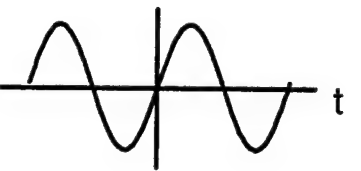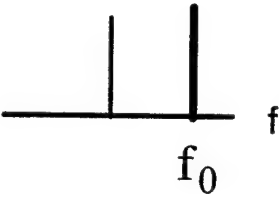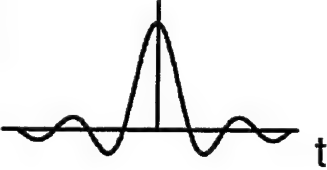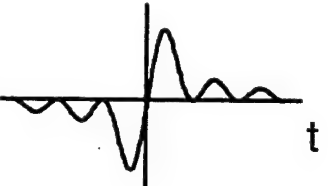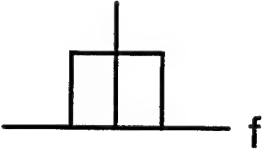| SIGNAL TRANSFORM	HILBERT TRANSFORM	FOURIER
$\cos\ (2\pi\ f_o\ t)$	$\sin\ (2\pi\ f_o\ t)$	
$\dfrac{\sin t}{t}$	$\dfrac{1-\cos t}{t}$	

Figure 3.1. Some examples of Hilbert Transform.

16

IV. DATA ANALYSIS

In this chapter we present the procedure and the results of the analysis of the Hamlet's Cove I surface wave data. The main goal is to determine if there is any phase correlation between data at the three buoys after low pass filtering and applying the Hilbert transform to the filtered data. Phase correlations can provide valuable information because they can tell us if the signal recorded from the three buoys corresponded to the same wave and if so, they can yield directly the phase velocity of the wave. Phase velocity is obtained by interpolating the correlation time between the buoys for which the location is known.

The data analyzed is of pressure measurements from a pressure gauge and two orthogonal components of velocity from a current meter. Because pressure gauge measurements are more sensitive to long waves, we will consider the low pass filtered output from for pressure gauge of measurements on 16 July 1994.

A. THE CHEBYSHEV TYPE II FILTER

An optimal filter needs to maintain amplitude information with no phase distortion in the pass band. In our case, the latter requirement is particularly important because from our approach, phase velocity values can only be determined from phase correlations. Because the filtering process should

minimize distortion of all small amplitude fluctuations, the stop band has to be at least 40 dB below the pass band to eliminate possible leakage problems and it has to have a minimum transition width to ensure good frequency separation. Most of these requirements can be met by with a Chebyshev type II filter. Higher order filters could introduce numerical errors, so the filter has to meet the requirements with the lowest order possible.

As shown in the Appendix (mfile), we used Matlab Signal Processing Toolbox (Mathworks, 1994). Of the two techniques, Analog Prototyping and Direct Design, we chose Analog Prototyping because the Direct Design technique has very stringent numerical accuracy constraints.

The Analog Prototyping technique allows the construction of digital equivalents of certain classical analog filters, especially Butterworth, Bessel, Chebyshev, and Elliptic. Among them and for ours purpose the Chebyshev Type II filter has the narrower transition and the flatter pass band response needed for the analysis of the data.

Analog filters are IIR (infinite-duration impulse) type filters, which necessarily introduce phase distortion. In order to overcome this problem the data was filtered both directions, forward and reverse by using the Matlab function *filtfilt* (Mathworks, 1994). With this approach, we can get precise zero-phase distortion and doubling of the filter order. Also, filtfilt minimizes startup and ending transients by adjusting initial conditions.

B. THE XCORRELATION FUNCTION

Matlab's function *xcorr* estimates the cross-correlation sequence of random processes. For the purpose of determining phase velocity values from apparently random time series, the cross-correlation function is important because it can provide a measure of the similarity between two signals.

The *xcorr* function can calculate the cross-correlation between two arrays of vectors of the same length, the autocorrelation for a vector, and the cross-correlation for a matrix. In all these forms of *xcorr*, the zero lag of the output is in the middle of the sequence. In order to normalized the sequence we used the option '*coeff*' so the autocorrelations at zero lag are identically 1.0.

C. PROCEDURE AND RESULTS

Figure 4.1 shows the Fourier transform of the pressure time series for the three buoys. From the shape of the spectrum, we can conclude that waves due to the local wind may correspond to frequencies above 0.1 Hz. If phase velocity values can be used to determine local bathymetry, waves generated by the local wind are unwelcome noise for the purpose of our analysis. Instead, the longer waves in the swell may characterize the bathymetry more accurately because of their direct response to the bottom topography manifested by refraction and diffraction effects. Swell may correspond to frequencies below 0.08 Hz, which we chose as the cutoff frequency for the low pass band of the filter.
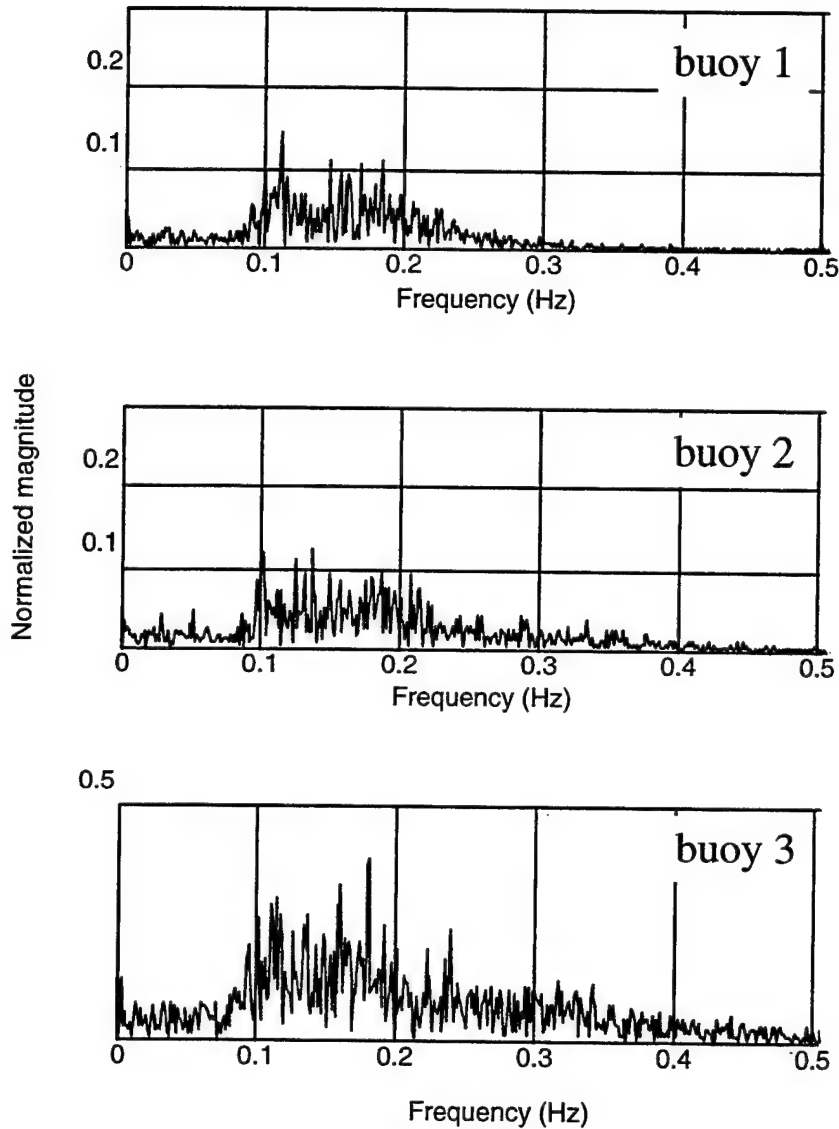
Figure 4.1. FFT of the pressure data for the three buoys. Frequencies above 0.1 Hz may correspond to waves generated by the local wind as evidenced by the increase of spectral energy and range.

With this information in mind, we filtered the whole time series using a

Chebyshev Type II filter with a cut off frequency of 0.08 Hz. Because of the

Chebyshev Type II filter introduces phase distortion, the wave data was filtered

in both the forward and reverse directions using the MATLAB function *filtfilt*, thus

20

obtaining precise zero-phase distortion and doubling of the filter order. As mentioned before, *filtfilt* minimizes startup and ending transients by adjusting initial conditions.

We applied the Hilbert transform to the filtered time series. Figure 4.2 shows the Matlab Power Spectrum function *(PSD)* of unfiltered time series and the *PSD* of the Hilbert transform of the data from the first buoy after filtering. Apparent from the figure, is that the power spectrum of the unfiltered data does not exhibit very good frequency-energy decomposition. On the other hand, the power spectrum of the Hilbert transform of the filtered time series shows good frequency-energy decomposition and enhancement of the more energetic waves of the filtered time series.

The data from each buoy has 172,800 points corresponding to two data point per second in a full day. Because this large array is numerically very demanding, we chose to work with a window of two hours, or 10% of the whole data. We applied Matlab's *Hilbert transform* ($\xi(t)$) function to the filtered data in this time window.   Along with the real time series (Y1), MATLAB generates the analytical signal

$$Z(t) = Y1(t) + i\xi\ (t)\ ,$$ (4.1)

which is similar to Eq. (3.2).
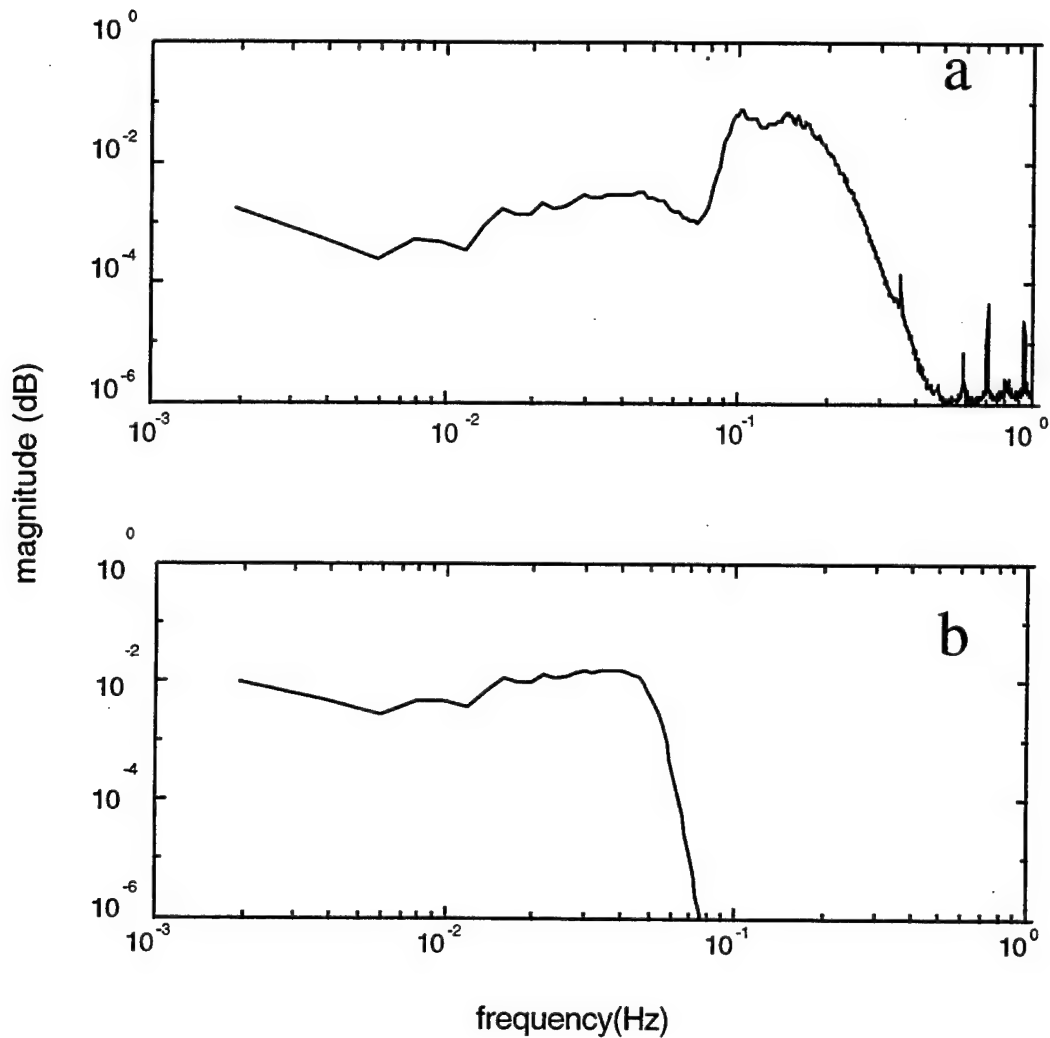
Figure 4.2. a) Power spectrum density for the pressure data at buoy 1 without filtering. b) Power spectra density of the Hilbert transform after low pass filtering using a Chebyshev type II filter with a 0.08 cutoff frequency.

Matlab's functions *angle* and *unwrap* (phase in radians 2*pi wrap), provide the phase of the time series (4.1). Shown in Figure 4.3 are the graphs corresponding to the phase of the whole pressure data from buoy 1 and also for the two hours window.
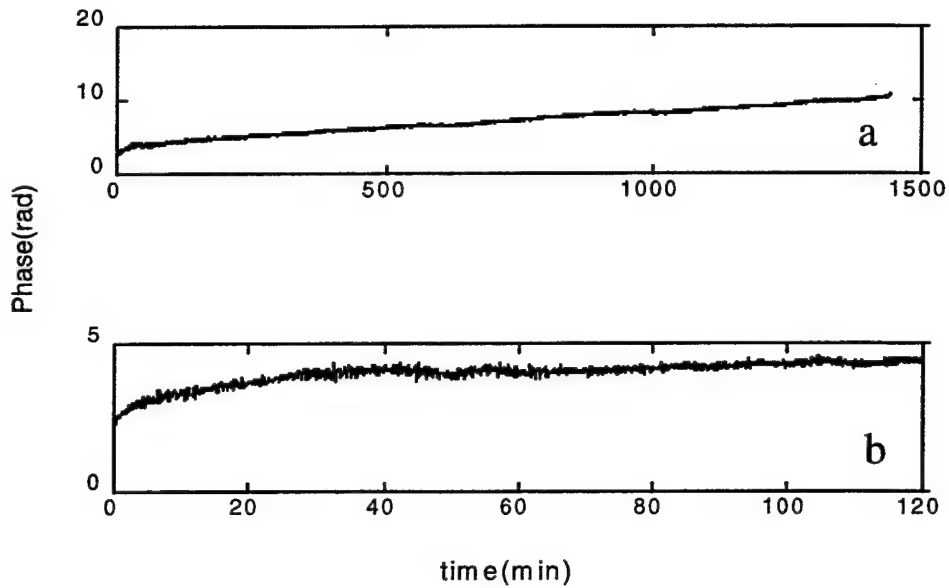
Figure 4.3. Phase (rad) as a function of time (min) for the pressure data at buoy 1 for a) one day, b) two hours.

The local frequency is by definition the slope of the phase and we applied to the phase data the MATLAB function *diff* and divided by the time between points (called tbp in Appendix) to get this slope. Figure 4.4 shows a plot of the local frequency as a function of time obtained from the data shown in Figure 4.3.
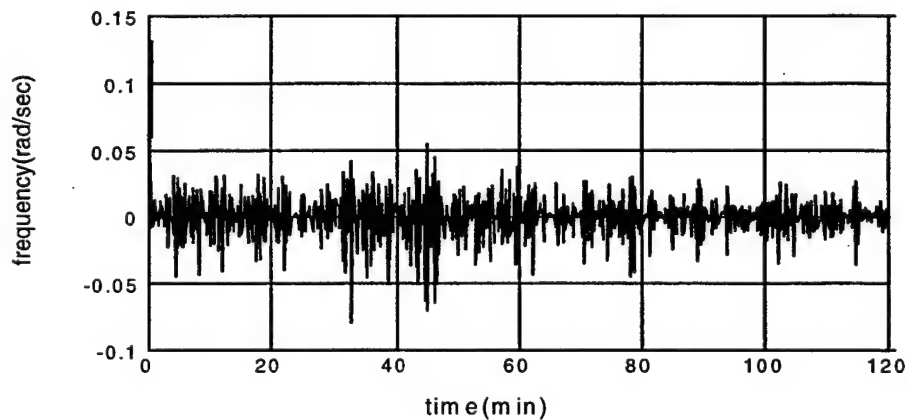
Figure 4.4. Local angular frequency as a function of time for buoy 1 for a two hour time window.

23

Figure 4.5 shows the cross-correlation of data from buoys 1, 2, and 3 using the *xcorr* function in MATLAB. The cross-correlation is blown-up in Figure 4.6. At the maximum of the cross-correlation we can obtain the time when the signals from two different buoys are highly correlated. Using this time, and knowing the distance between buoys, we can estimate the phase velocity at which the wave is moving from one buoy to the other. Assuming that the three buoys started to record the data at the same time, we get the phase velocities estimates shown in Table 4-1.
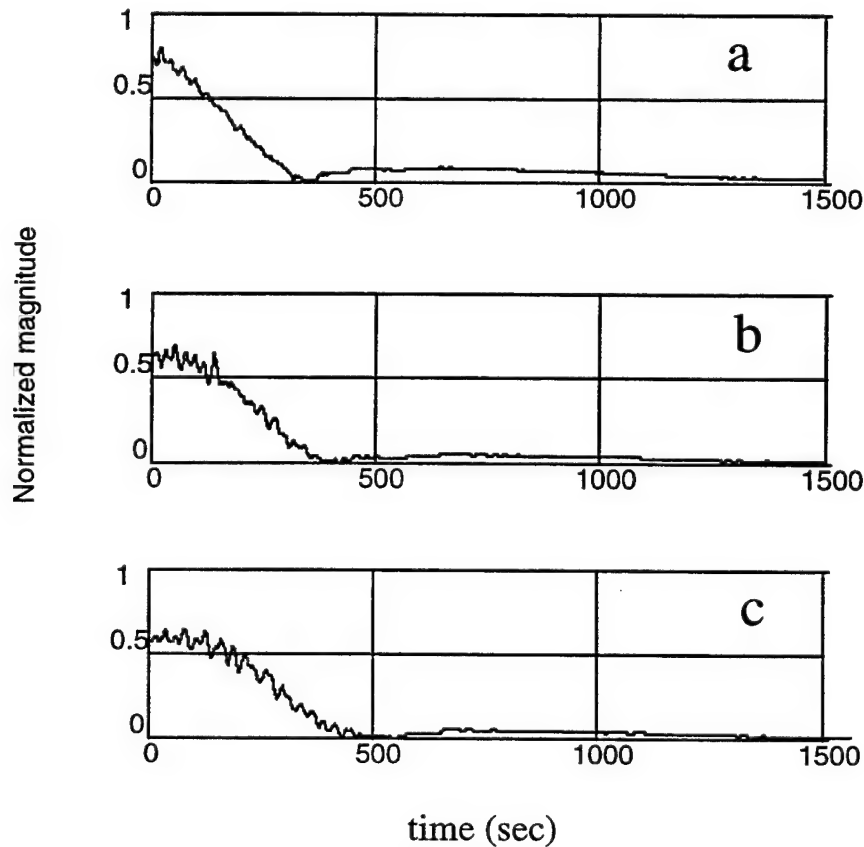
Figure 4.5. Cross correlation of the phase between a) buoys 1 and 2, b) buoys 1 and 3, and c) buoys 3 and 2.

24
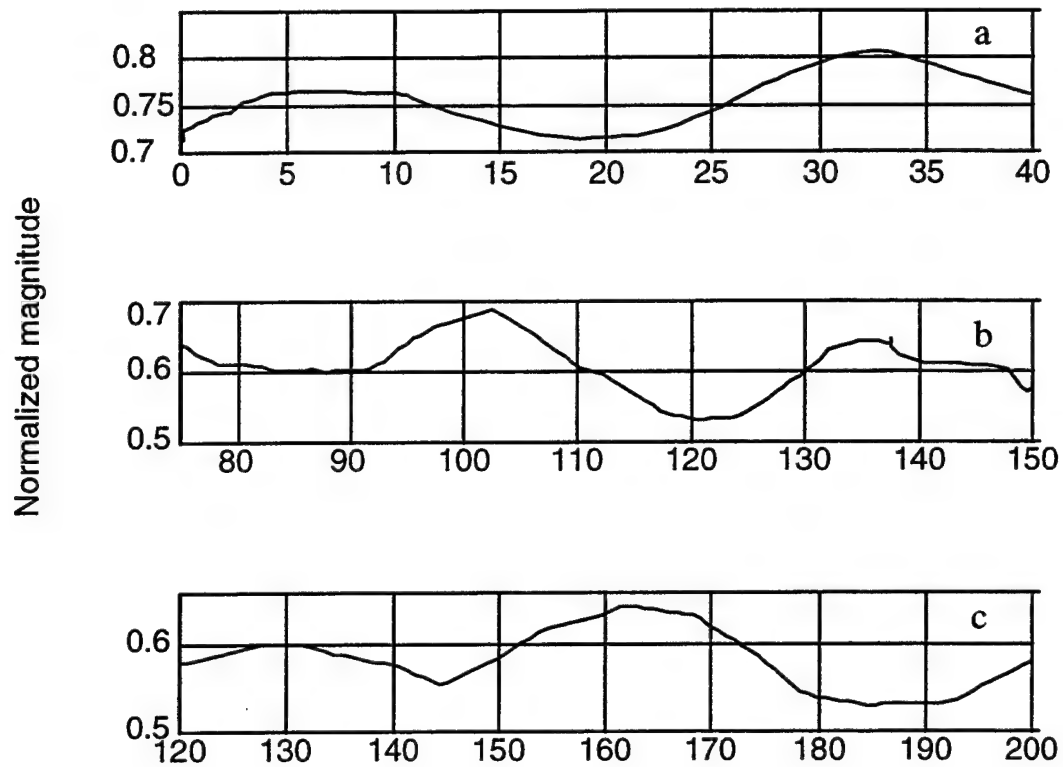
Figure 4.6. Blown up of the cross correlations in Figure 4.5.

	distance	correlation time	calculated phase velocity
Buoy 1 - Buoy 2	123.46 m	34 s	3.63 m / s
Buoy 2 - Buoy 3	219.16 m	163 s	1.35 m / s
Buoy 1 - Buoy 3	342.62 m	102 s	3.36 m / s

Table 4-1. Relations of the distances among the buoys, correlation time and phase velocity.

V. DISCUSSION OF RESULTS AND RECOMMENDATIONS FOR FUTURE WORK

We have investigated the Hilbert transform as a tool to determine phase velocity from ocean wave data of three buoys. The values tabulated in Table 4-1 were obtained by dividing the distance between buoys by the time for maximum phase correlation of the time series of pressure measurements at the corresponding buoys.

Table 5-1 is a comparison between the values of phase velocity as determined by the correlation times to the values of phase velocity assuming linear shallow water theory over uniform bottom topography. The value of the phase velocity determined from shallow water theory represents an upper bound. If the normal to the wave front makes an angle with the line joining two buoys, the value of phase velocity obtained from correlations of the time series will yield an underestimation. Thus, the low values obtained from the correlations may be due, in part, to an effective average over all possible directions.

|	phase velocity from correlations	average depth	calculated phase velocity
Buoy 1 - Buoy 2	3.63 m/s	6.10 m	7.73 m/sec
Buoy 2 - Buoy 3	1.35 m/s	3.81 m	6.11 m / sec
Buoy 1 - Buoy 3	3.36 m/s	5.34 m	7.23 m / sec

Table 5.1 Comparison of phase velocity values determined from correlations (second column) and from shallow water theory (fourth column) assuming uniform depth (third column).

27

It is then apparent that to accurately determine the phase velocity from time series, we require an accurate directional spectral data or surface height time series from a bigger array of buoys. An accurate directional spectra provides the necessary angular information that can be used to determine the true value of the phase velocity. As shown by Rikiishi (1978) time series from a minimum of three buoys cannot be used to determine directional spectra for a broadband distribution of waves.

Any data analysis on time series from pressure gauge measurements have fundamental limitations. First, because the pressure gauge responds to the rise and fall to the free surface, the pressure at depth z attenuates by a factor proportional to e^{-kz} where k is $2\pi/\lambda$ and λ is the wavelength of the Fourier component of the surface disturbance. Unless the wave data corresponds exclusively to shallow water, the correlation time determined from the phase of the Hilbert transform at two points may be inaccurate. Second, if the wave field is nonlinear, the pressure and the surface height are nonlinearly related. Due to nonlinearities, the correlation time from pressure gauge measurements may yield misleading phase velocity results. Thus, phase velocity values from phase correlations using the Hilbert transform, are more reliable with time series of surface height measurements.

If the deficiencies noted above can be corrected, the preliminary results of this thesis are evidence of the powerful technique of using Hilbert transform to determine the phase velocity of low frequency shoaling waves. This technique can be summarize operationally as follows. The analytic signal of a time series

28

possesses a natural phase. Correlations of the phase yield an average time of travel. If directional spectra are available, the angular information can then yield the true time of travel from which the phase velocity can be determined. In this approach, there is no explicit assumption of the relation between frequency and wavenumber of waves in the wave field, indicating that it may be applicable to arbitrary wave fields, both linear and nonlinear.

APPENDIX MATLAB CODE

This appendix contains the particular mfile (Matlab Code) that we used to analyze the data from the three buoys in order to extract the information that we were interesting on.

```
%Loading the desired data
load 16jul1a.dat              ;
p1=16jul1a(:,1)              ;
clear 16jul1a                ;
load 16jul2a.dat              ;
p2=jul2a(:,1)                ;
clear 16jul2a                ;
load 16jul3a.dat              ;
p3=16jul3a(:,3)              ;
clear 16jul3a                ;
p1=p1-mean(p1)               ;
p2=p2-mean(p2)               ;
p3=p3-mean(p3)               ;
fs=2                         ; %Sampling frequency
M1= max(size(p1))            ; %Get Number of data points
N=172800                     ; %Total number of points
f=0:fs/N:(N-1)*(fs/N)        ; %Normalizing the x-axis to frequency
tbp=0.5                      ; %Time between data points in seconds
t1=[1:M1].*(tbp/60)          ; %Normalizing the x-axis to time in minutes
```

% Looking for the FFT of the data from the three buoys to select the desired frequencies

```
P1=fft(p1)*2/length(p1)      ;
P2=fft(p2)*2/length(p2)      ;
P3=fft(p3)*2/length(p3)      ;
```

% Applying the filter and Hilbert Transform to the data

```
cf_low=0.08                   ; %cut off frequency for buoys 1,2 and 3.
[b1,a1]=cheby2(5,40,cf_low/(fs/2));%Chebyshev filter 5 order 40 dB for data
                              %form buoy 1
```

31

```
Y1=filtfilt(b1, a1, p1)              ; %Filtering data from buoy 1
clear p1                             ; %Clear data pressure 1 from memory
V_wavep1=hilbert(Y1)                 ; %Hilbert Transform data from buoy 1
phasep1=angle(V_wavep1)              ; %Phase of the Hilbert Transform for buoy 1
[S1,f1]=psd(Y1,1024,fs)              ;%examine spectrum of the low wave
                                       %without filtering
[S2,f2]=psd(V_wavep1,1024,fs)        ;%examine spectrum of the low wave
                                       %after filtering and the Hilbert transform
[b2,a2]=cheby2(5,40,cf_low/(fs/2)); %Chebyshev filter order 5 , 40 dB.
Y2=filtfilt(b2, a2, p2)              ;%Filtering data from buoy2
clear p2                             ; %Clear data pressure 2 from memory
V_wavep2=hilbert(Y2)                 ; %Hilbert Transform data from buoy 2
phasep2=angle(V_wavep2)              ; %Phase of the Hilbert Transform for buoy 1
[b3,a3]=cheby2(5,40,cf_low/(fs/2)); %Chebyshev filter for data from buoy 3
Y3=filtfilt(b3, a3, p3)              ; %Filtering data from buoy 3
V_wavep3=hilbert(Y3)                 ; %Hilbert Transform data from buoy 3
phasep3=angle(V_wavep3)              ; %Phase of the Hilbert Transform for buoy 1
clear p3                             ; %Clear data pressure 3 from memory
```
%Looking in a two hours windows of the data for each buoy
```
V_wavep1=V_wavep1(1:14400)  ; %points correspond to a two hours   windows
V_wavep2=V_wavep2(1:14400)  ; %points correspond to a two hours windows
V_wavep3=V_wave p3(1:14400) ; %points correspond.to a two hours windows
Y1=Y1(1:14400)              ; %points correspond to a two hours windows
Y2=Y2(1:14400)              ; %points correspond to a two hours windows
Y3=Y3(1:14400)              ; %points correspond to a two hours windows
t1=t1(1:14400)              ; %Two hour time window
```
%Looking for the phase of the Hilbert Transform for the two hour window
```
theta1=unwrap(angle(V_wavep1)); %Phase of the Hilbert transform in radians
theta2=unwrap(angle(V_wavep2)); %Phase of the Hilbert transform in radians
theta3=unwrap(angle(V_wavep3)); %Phase of the Hilbert transform in radians
```
%Looking for the derivative of the phase of the Hilbert Transform for the two hour window
```
dtheta1 = diff(theta1./tbp)          ; %By definition the Local frequency at
```

32

```
                                          %buoy 1

dtheta2 = diff(theta2./tbp)               ;%By definition the Local frequency at

                                          %buoy 2

dtheta3 = diff(theta3./tbp)               ;%By definition the Local frequency at

                                          %buoy 3

%Looking for the cross-correlation of the phase of the Hilbert transform

Cp21=xcorr(phasep2, phasep1,'coeff')      ;%Xcorrelations of the phase of the

                                          %signal from Buoy 2 and 1.

Cp31=xcorr(phasep3, phasep1,'coeff')      ;%Xcorrelations of the phase of the

                                          %signal from Buoy 3 and 1.

Cp32=xcorr(phasep3, phasep2,'coeff')      ;%Xcorrelations of the phase of the

                                          %signal from Buoy 3 and 2.

Cps21=fftshift(Cp21)                      ; %Shift of the correlations

Cps31=fftshift(Cp31)                      ; %Shift of the correlations

Cps32=fftshift(Cp32)                      ; %Shift of the correlations

%Plots of the FFT of the data pressure from the three buoys

subplot (3,1,1)

plot(f,abs(P1)),axis([0 0.5 0 0.05]),grid,title('FFT of Data Pressure

of buoy 1 vs Frequency'),

subplot (3,1,2)

plot(f,abs(P2)),axis([0 0.5 0 0.05]),grid,

title('FFT of Data Pressure of buoy 2 vs Frequency'),
```

```
subplot (3,1,3)

plot(f,abs(P3)),axis([0 0.5 0 0.05]),grid,

title('FFT of Data Pressure of buoy 3 vs Frequency'),

xlabel('Frequency'),ylabel('Normalized magnitude')     ;

clear P1; clear P2; clear P3                    ;%Release memory
```

%**Plot of the Power Estimate Spectrum**

```
figure; clf;

subplot(2, 1, 1)

loglog(f1,S1),axis([1E-3 1 1E-6 1]);

title('Power spectrum Estimate of Pressure data frequency without filtering');

ylabel('magnitude (dB)');

subplot(2, 1, 2)

loglog(f2,S2),axis([1E-3 1 1E-6 1]);

title('Power spectrum Estimate of V_wavep1 after Hilbert Transform  ');

xlabel(['frequency(Hz)-cutoff frequency',num2str(cf_low),'Hz']);

ylabel('magnitude (dB)');
```

%**Plot of the Phase in radians (Unwrap) of the Hilbert transform**

```
figure; clf;

subplot(3, 1, 1)

plot(t1,(phase_1)),

title('Plot of the phase of Hilbert Transform of the pressure data buoy 1');

xlabel('time(min)'); ylabel('Phase(rad)');
```

34

```
subplot(3, 1, 2)

plot(t1,(phase_2)),title('Plot of the phase of Hilbert Transform of the pressure
data buoy 2'); xlabel('time(min)');ylabel('Phase(rad)');

subplot(3, 1, 3)

plot(t1,(phase_3)),title('Plot of the phase of Hilbert Transform of the pressure
data buoy 3'); xlabel('time(min)'); ylabel('Phase(rad)');
```

%Plots of the Local frequency as a function of the time, data from buoy 1

```
figure; clf;

plot(t1,dtheta1); title('Plot of the Local Frequency as a function of time at buoy
1'); xlabel('time(min)'); ylabel('frequency(rad/sec)');
```

%Plots of the correlations of the data of the three buoys

```
figure;clf;

subplot(3, 1, 1)

plot(t1,abs(Cp21)),grid,title('Correlation of Phase of the data from Buoy 2 and
Buoy 1'),xlabel('Time(sec)') ;

subplot(3, 1, 2)

plot(t1,abs(Cp31)),grid,title('Correlation of  Phase of the data from Buoy 3 and
Buoy 1'),xlabel('Time(sec)');

subplot(3, 1, 3)

plot(t1,abs(Cp32)),grid,title('Correlation of  Phase of the data from Buoy 3 and
Buoy 2'),xlabel('Time(sec)');
```

%Plot of the shift of the correlations of the Phase from the three buoys

```matlab
figure;clf;

subplot(3, 1, 1)

plot(t1,abs(Cps21)),grid,title('Shift of Correlation of  Phase of the data from Buoy

2 and Buoy 1'),axis([0 1500 0 1]);

subplot(3, 1, 2)

plot(t1,abs(Cps31)),grid,title('Shift of Correlation of  Phase of the data from Buoy

3 and Buoy 1'),axis([0 1500 0 1]);

subplot(3, 1, 3)

plot(t1,abs(Cps32)),grid,title('Shift of Correlation of  Phase of the data from Buoy

3 and Buoy 2'),axis([0 1500 0 1]);
```

%Plot of the Maximum values of the shifted correlations

```matlab
figure;clf;

subplot(3, 1, 1)

plot(abs(Cps21)),grid,title('Max. value of the Correlation of the  Phase of the data

from Buoy 2 and Buoy 1'),axis([0 40 0.7 0.85]);

subplot(3, 1, 2)

plot(abs(Cps31)),grid,title('Max. value of the Correlation of the  Phase of the data

from Buoy 3 and Buoy 1'),axis([75 150 0.5 0.7]);

subplot(3, 1, 3)

plot(abs(Cps32)),grid,title('Max. value of the Correlation of the  Phase of the data

from Buoy 3 and Buoy 2'),axis([120 200 0.5 0.66]);
```

REFERENCES

M. Abreu, A. Larraza, and E. Thornton, 1992. "Nonlinear transformation of directional wave spectra in shallow water," J. Geophys. Res. **97**, 15,579-15,589.

D. J. Acheson, 1995. "Elementary Fluid Dynamics" Clarendon Press. Oxford, 78-80.

T. Akal, 1980. "Sea Floor Effects on Shallow-water Acoustic Propagation". In: Bottom-interacting Ocean Acoustics ." Eds.: Kuperman, W. A. and Jensen, F. B. Plenum Press , New York.

T. Akal, and F. Jensen, 1983."Effects of the Sea-bed on Acoustic Propagation. In: Acoustic and the Sea-bed ." Eds.: Pace, N. R. Bath University Press, 225.

J. Bendat, 1989. "The Hilbert Transform and Applications to Correlations Measurements" Independent Publication, 4-37.

B. Boashash, 1992. "Time-Frequency Signal Analysis Methods and Applications," Longman Cheshire, 163-232.

M. H. Freilich and R. T. Guza, 1984. "Nonlinear effects on shoaling surface gravity waves," Phil. Trans. R. Soc. Lond. A **311**, 1-41.

Matlab Reference Guide, 1992. The Mathworks Inc., Natick, MA.

A. Larraza, 1994. "A path integral approach to shoaling waves," preprint.

P. L. Liu, S. B. Yoon, and J. T. Kirby, 1985. "Nonlinear refraction-diffraction in shallow water," J. Fluid. Mech., **153**, 185-209.

S. Long, N. Huang, T. Chi-chao, M. Wu, E. Mollo_Christensen, and Y. Yuan, 1995. "The Hilbert Techniques: An Alternate Approach For Non-Steady Time Series Analysis," IEEE Geoscience and Remote Sensing , 6-11 .

K. Rikiishi, 1978. "A new method for measuring the directional spectrum. Part I. Description," J. Phys. Ocean., **8**, 508-517.

P. Smith, 1994. "Hamlet's Cove Quick Look In-Water Ground Truth Report" Naval Research Laboratory, Code 7240, Stennis Space Center.

Signal Processing Toolbox User's Guide, 1993 .The Mathworks Inc., Natick, MA.

S. D. Stearns, R. A. David,1987 "Signal Processing Algorithms" Prentice-Hell,

Inc. 140-144.

INITIAL DISTRIBUTION LIST

No. of Copies

1. Defense Technical Information Center 2
   8725 John J. Kingman Rd. STE 0944
   Ft. Belvoir, VA 22060-6218

2. Dudley Knox Library 2
   Naval Postgraduate School
   411 Dyer Rd.
   Monterey, CA 93943

3. Chairman, Code PH/Lv 1
   Physics Department
   Naval Postgraduate School
   Monterey, CA 93943

4. Prof. Andrés Larraza, Code PH/La 2
   Physics Department
   Naval Postgraduate School
   Monterey, CA 93943

5. Prof. Roberto Cristi, Code EC/Cx 1
   Department of Electrical Engineering
   Naval Postgraduate School
   Monterey, CA 93943

6. Comandancia General de la Armada 1
   Jefatura de Educación
   Av. Vollmer, San Bernardino
   Caracas, 1011. Venezuela

7. CC. Moisés Navarro López 1
   Comandancia General de la Armada
   Av. Vollmer, San Bernardino
   Caracas, 1011. Venezuela